Astron. Astrophys. 285, 609–620 (1994)

ASTRONOMY
AND
ASTROPHYSICS

The Wilson-Bappu effect and other Ca II H and K line parameters relationships in chromospherically active binaries

D. Montes, M.J. Fernández-Figueroa, E. De Castro, and M. Cornide

Departamento de Astrofísica, Facultad de Físicas, Universidad Complutense de Madrid, E-28040 Madrid, Spain
SPAN: 16555::EUCMVX::ELIC

Received 29 July 1993 / Accepted 6 November 1993

Abstract. We present measurements of the emission core width W_0 and the wavelength separation of the K_1 dips, W_1, of the Ca II H and K emission lines observed on high-dispersion spectra of 28 chromospherically active binary systems (RS CVn and BY Dra stars) and 18 single active stars. We test the width-luminosity correlations (the Wilson-Bappu (WB) effect, and (W_1, M_V)) in these very active stars and analyse the influence of the activity level (I_{K_3}) and the rotational broadening (V sin i) in these correlations.

We have found that for very active stars the emission widths, both W_0 and W_1, are larger than expected from previously accepted width-luminosity relations. The stars with strong emission intensities, I_{K_3}, and large values of V sin i seem to present larger values of W_0 than resulted from WB relation, the effect of the rotational velocity being the most remarkable. On the contrary, W_1 is strongly influenced by I_{K_3} but the effect of the rotational broadening is lesser.

We also analyse the behaviour of the Ca II H and K line parameters in these very active stars in relation with less active stars and we found that the increase of W_1 and I_{K_1} with I_{K_3} presents a flattening for the most active stars which is different for each value of W_0.

Finally we also find a Hϵ width-luminosity correlation in the stars of the sample in which this emission line is present.

Key words: stars: activity – stars: binaries: close – stars: chromospheres – stars: distances – stars: late-type – stars: rotation

1. Introduction

One of the most remarkable properties of the Ca II K emission core (Fig. 1) is the correlation between the width, W_0(K), and the stellar absolute visual magnitude, M_V. This correlation is known as the Wilson-Bappu effect (Wilson & Bappu 1957, hereafter WB) and seems to represent a fundamental relationship between some chromospheric property and the global parameters of the underlying star. The Wilson-Bappu effect is remarkable for three reasons: (1) The width-luminosity law is obeyed over a wide ($\sim 10^5$) range of stellar luminosity. (2) The emission width appears to be independent of core emission strengths. (3) The widths are not strongly correlated with stellar metallicity. The physical meaning of the Wilson Bappu effect is still unclear, although many theoretical interpretations have been proposed and several authors have expressed the line widths empirically in terms of fundamental stellar parameters. The relation between W_0 and the effective temperature T_{eff}, the surface gravity g and the metal abundance [Fe/H] has been investigated by Reimers (1973), Neckel (1974) and Lutz & Pagel (1982). Two alternative types of explanation of the WB effect have been reported:

a) Those based on a systematic effect in the doppler broadening (Athay & Skumanich 1968; Linsky & Avrett 1970; Fosbury 1973; Scharmer 1976)

b) Those based on a systematic effect in the column mass density above the temperature minimum leading to a spread in the optical depth profile in the damping wings. (Thomas 1973; Ayres et al. 1975; Engvold & Rygh 1978; Ayres 1979)

On the other hand, the influence of the intensity of the emission Ca II K line (I_{K_3}) in the WB width, W_0, has been studied by Glebocki & Stawikowski (1978) and the effect of the rotational broadening (V sin i) in the Ca II K line was analysed by Bielicz et al. (1985). Furthermore Neckel (1974) also suggested that the evolutionary status (age) of the stars must be taken into account.

In this paper we analyse the WB effect in a sample of chromospherically active binary systems (RS Canum Venaticorum (RS CVn) and BY Draconis (BY Dra) systems) and in some moderately and highly active single stars. The main purpose of the present analysis is to investigate qualitatively if these very active and rapidly rotating stars deviate significantly from the WB law. In particular we investigate what is the influence of the level of activity throughout the intensity of the K_3 feature, (I_{K_3}) and the rotational broadening (V sin i) in the width-luminosity correlations (log W_0, M_V) and (log W_1, M_V). We also analyse the behaviour of the Ca II H and K line parameters in these very

Send offprint requests to: M.J. Fernández-Figueroa

Table 1. Summary of the observations.

O	Date	Telescope	Å/pixel	FWHM(inst)
1	1985 June	INT	0.100	0.200
2	1986 November	CAHA	0.200	0.400
3	1987 June	INT	0.100	0.200
4	1988 January	CAHA	0.099	0.198
5	1988 July	INT	0.099	0.198
6	1989 July	CAHA	0.099	0.198
7	1991 October	INT	0.190	0.380
8	1992 December	INT	0.179	0.358
9	1993 March	CAHA	0.210	0.420

active stars in comparison with less active stars and the influence of W_0 width in these parameters.

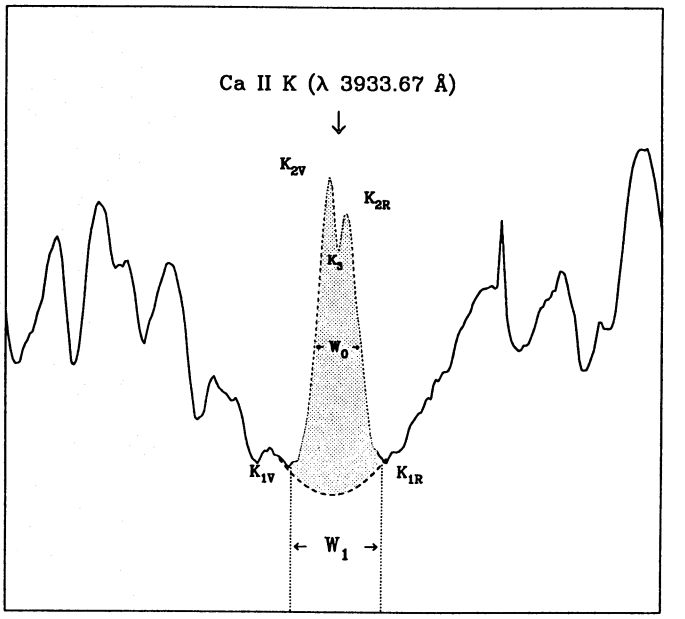

Fig. 1. Description of the Ca II K line parameters

2. Observational data

2.1. Observations

High resolution observations of the Ca II H and K lines have been carried out in several runs on two telescopes:

– 2.2m Telescope at the German Spanish Astronomical Observatory in Calar Alto (CAHA; Almería, Spain), using the coudé spectrograph and a CCD as detector.

– Isaac Newton Telescope (INT) at the Observatorio del Roque de los Muchachos (La Palma, Spain), using the IDS and an IPCS or a CCD as detectors.

The spectra have been extracted from the CCD images using standard procedures (bias subtraction and flat-field correction) and wavelength-calibrated using the MIDAS package.

The reciprocal dispersion achieved and the full width at half maximum (FWHM) of the instrumental profile corresponding to each observing run are given in Table 1.

2.2. The sample of stars

In this study stars with different levels of activity are included. These can be divided into three groups:

i) *Chromospherically active binary systems*

In this group we include 27 chromospherically active binary systems (RS CVn and BY Dra stars) observed by us in the Ca II H and K lines region and included in the catalog of chromospherically active binary stars by Strassmeier et al. (1988) (hereafter CABS I) and the second edition by Strassmeier et al. (1993) (hereafter CABS II). We analyse here only the systems in which the active component has the main contribution to the observed spectrum, i.e. the emission line and the absorption profile correspond to the same star. This constrains the number of systems which can be analysed but it allows to obtain real measurement of widths and intensities (W_0, W_1, I_{K_1}, and I_{K_3}).

The behaviour of the Ca II H and K lines have been studied by us in a large number of systems (Fernández-Figueroa et al. 1993). The HD number, the name and spectral type (T_{sp}) from CABS II, of these systems are given in Table 2.

ii) *Single active stars*

In this group we include 18 single active stars of spectral types F, G and K, some of them contained in the sample of Wilson (1978). We include here only the stars observed by us in which the intensity of Ca II H and K emission lines permits to obtain reliable measurements of the line parameters. The name, HD number, and spectral type (T_{sp}) of these systems are given in Table 3.

iii) *Barium stars and other giants*

To increase the range of stellar luminosities we include several giant and supergiant stars studied by us in a previous work (Cornide et al. 1992). The stellar parameters of these systems (9 Barium stars, and 3 normal giants) are given in Table 4.

2.3. Visual absolute magnitudes M_V

We have adopted visual absolute magnitudes based on the most reliable trigonometric parallaxes. These absolute magnitudes are completely independent of particular spectroscopic features, which is essential in this study.

For the chromospherically active binary systems we have adopted the trigonometric parallaxes, π, and the visual magnitudes, V, reported in CABS II. For the single active stars and the Barium stars the parallaxes, π, were taken from the Bright Star Catalogue (Hoffleit & Jaschek 1982). We adopted new determinations of trigonometric parallaxes (π * in Tables 2, 3 and 4) reported by Van Altena et al. (1991) (The General Catalogue of Trigonometric Parallaxes, preliminary version) when they were available.

In Tables 2, 3 and 4 $M_V(\pi)$ is the absolute magnitude obtained with V and π (or π * when available) and $M_V(T_{sp})$ is the absolute magnitude corresponding to the spectral type from Landolt-Börnstein (Schmidt-Kaler 1982).

2.4. *Ca II H and K line parameters*

The Ca II H and K lines of active stars have a characteristic profile of a collisional dominated resonance line. In this profile it is possible to distinguish three features, see Fig. 1.

K_1 : The broad deep absorption feature produced in the photosphere.

K_2 : The sharp emission peak produced in the chromosphere in a layer immediately above the photosphere.

K_3 : The self-reversal core produced at the top of the chromosphere at a height from which the photons at the line center can escape.

The violet and red individual turning points in the Ca II K emission profile are denoted as: K_{1V}, K_{1R}, K_{2V}, K_{2R}.

The Wilson-Bappu width, W_0, is measured as the full width at half intensity between the K_1 and K_2 features, while W_1 is the full width of the emission core ($W_1 = \Delta K_1 = \lambda_{K_{1R}} - \lambda_{K_{1V}}$), and W_2 is the separation between the blue and red peaks within the emission profile ($W_2 = \Delta K_2 = \lambda_{K_{2R}} - \lambda_{K_{2V}}$).

The above Ca II K line signatures can be characterized with their corresponding intensities $I_{K_{1V}}$, $I_{K_{1R}}$, $I_{K_{2V}}$, $I_{K_{2R}}$ and I_{K_3}. For the Ca II H line similar parameters are defined.

The measured Ca II H and K line parameters, corresponding to the groups i), ii) and iii) are given in Tables 5, 6 and 7 respectively. All the line widths are expressed in Å and are not corrected for instrumental broadening. Moreover, the line intensities have been measured in the spectra normalised to the 3950.5 Å pseudocontinuum.

Column (3) of Table 5 gives the orbital phases (φ) for each measured spectra of group i) and, in column (4), H and C stand for emission belonging to hot and cool component respectively. The columns heading with O in Tables 5, 6 and 7 list a code for the date, telescope, and spectral resolution as explained in Table 1.

For stars belonging to groups i) and ii) it is not possible to observe the self-reversed core K_3 (except in V1764 Cyg and o Dra) either because we have not enough spectral resolution or/and because the K_2 separation is very small due to the high activity level of these stars (Ayres 1979). Therefore, in these stars it is not possible to measure the parameters, $I_{K_{2V}}$, $I_{K_{2R}}$, and W_2 and the measured I_{K_3} intensity is equal to I_{K_2} intensity. For the stars of group iii) the self-reversed core is present and all the line parameters are given in Table 7.

3. The Wilson-Bappu relationship

Wilson & Bappu (1957) defined the width of the emission in the Ca II lines, W, as the wavelength difference between the red and violet edges of the emission, expressed in km s^{-1}.

Lutz (1970) has shown that W_0 is very nearly the full width at half maximum (FWHM) of the emission core.

Linsky et al. (1979) measured W as the sum of the half-widths at half-maximum of the red and violet emission features. This definition is equivalent to the usual definition of FWHM for symmetric emission lines, and it allows for a width measurement of those profiles that are very asymmetric.

In this work, W has been determined, as the FWHM of the emission core, from a Gaussian fit to the observed emission line profile in the case of symmetric lines, and following the definition of Linsky et al. (1979) in the case of asymmetric lines, i.e. when the self-reversed core is present in the observed profile.

3.1. *The corrected width W_0*

The measured width W must be corrected for the instrumental broadening. To correct their W measurements, Wilson & Bappu (1957) originally subtracted from them the projected slit width (15 km s^{-1}). Later, Wilson (1959) found that a correction of 18 km s^{-1} improved the linearity of the WB relationship.

Some authors (Wilson 1959; Linsky et al. 1979) suggested a simple formula for the instrumental width correction b, which is related to the true width W_0 by:

$$W_0 = W - b. \tag{1}$$

This correction is only strictly valid when W and b represent the FWHM of Lorentz profiles. However Lutz (1970) proposed a quadratic correction valid to Gaussian profiles:

$$W_0^2 = W^2 - b^2. \tag{2}$$

This author remarks that the linear correction used by Wilson usually gives a value of W_0 which is in error by a larger amount than the uncorrected width and that a quadratic correction gives a result which is closer to the true width than the linear correction, and its error is always smaller than that of the uncorrected width. Fosbury (1973) noted that, although the detailed form of the correction curve depends on the line shape, for all realistic profiles a Gaussian (quadratic) correction is a good approximation.

In this work we use a quadratic correction setting b parameter equal to the instrumental FWHM corresponding to each observing run (see Table 1). We have tested the linear and quadratic corrections and we have found that the scatter is lower with a quadratic correction, particularly in the case in which the measured width, W, is comparable to the instrumental width, b.

We have found a satisfactory agreement when we compare our corrected widths with previous values from different authors (Wilson & Bappu 1957; Stencel 1977; Linsky et al. 1979; Strassmeier et al. 1990; García-López et al. 1992). The small discrepancies are due to the different spectral resolution and correction procedures used.

3.2. *Proposed (log $W_0(K)$, M_V) relations*

Wilson (1959) obtained the following Sun-Hyades calibration:

$$M_V = -14.94 \log W_0(K) + 27.59. \tag{3}$$

Table 2. RS CVn and BY Dra stars parameters

HD	Name	T_{sp}	$V \sin i$ (km s^{-1})	V (mag)	π ($''$)	π * ($''$)	$M_V(\pi)$ (mag)	$M_V(T_{sp})$ (mag)	$M_V(K)_{WB}$ (mag)	$M_V(K)_{Our}$ (mag)
1833	BD Cet	K1III	20	7.89	0.0141	-	3.64	0.6	-1.39	0.02
4502	ζ And	/K1III	40	4.06	0.0323	0.0359	1.84	0.6	-1.62	-0.22
5516	η And	G8IV-III/G8IV-III	< 15	5.17	0.0090	0.0043	-1.66	2.0	-0.36	1.08
7672	AY Cet	WD/G5III	/4	5.47	0.0150	0.0163	1.53	0.9	1.78	3.29
8357	AR Psc	K2V/	9/6	7.24	0.0588	-	6.09	6.4	4.32	5.91
12545	-	K0III	17	7.6	0.0130	-	3.17	0.7	0.58	2.06
17433	VY Ari	K3-4V-IV	6	6.9	0.0476	0.0499	5.25	3.5	3.52	5.08
32357	12 Cam	K0III	25	6.1	0.0075	-	0.48	0.7	-1.73	-0.32
37824	V1149 Ori	K1III	11	6.58		-		0.6	-0.59	0.85
62044	σ Gem	K1III	29	4.14	0.0169	0.0178	0.39	0.6	-0.83	0.61
-	DM UMa	K0-1IV-III	36	9.55	0.0077	-	4.00	2.0	0.01	1.46
98230	ξ UMa(B)	G5V	2.8	4.87	0.1266	0.1305	5.45	5.1	4.82	6.42
113816	-	K2IV-III	30	8.27	0.0061	-	2.20	2.0	-1.15	0.27
136905	GX Lib	G-KV/K1III	32	7.29		-		0.6	-1.65	-0.25
153751	ϵ UMi	A8-F0V/G5III	25	4.23	0.0141	0.0090	-0.04	0.9	-2.34	-0.96
160538	DR Dra	WD/K0-2III	4	6.55	0.0114	-	1.83	0.6	0.44	1.91
166181	V815 Her	G5V/[M1-2V]	27/	7.66	0.0323	-	5.19	5.1	2.22	3.74
175306	o Dra	G9III	16	4.64	0.0149	0.0033	-2.77	0.8	-3.10	-1.73
175742	V775 Her	K0V/[K5-M2V]	15/	8.04	0.042	0.0421	6.16	5.9	2.50	4.03
178450	V478 Lyr	G8V/[dK-dM]	21/	7.68	0.0385	-	5.61	5.5	2.64	4.18
179094	V1762 Cyg	K1IV-III	14	5.81	0.0040	0.0040	-1.18	2.0	0.07	1.53
185151	V1764 Cyg	F/K1III	34	7.69	0.0026	-	-0.24	0.6	-4.40	-3.07
206301	42 Cap	G2IV	5.5	5.17	0.029	0.0294	2.56	3.0	0.38	1.85
209813	HK Lac	F1V/K0III	15	6.52	0.0067	-	0.65	0.7	-0.26	1.19
213389	V350 Lac	K2III	36	6.38	0.0145	-	2.19	0.5	-1.40	0.01
216489	IM Peg	K2III-II	36	5.60	0.0200	-	2.11	-1.1	-1.03	0.40
222107	λ And	G8IV-III	10	3.70	0.0435	0.0494	2.17	2.0	0.54	2.01

Table 3. Single active stars parameters

HD	Name	T_{sp}	$V \sin i$ (km s^{-1})	V (mag)	π ($''$)	π * ($''$)	$M_V(\pi)$ (mag)	$M_V(T_{sp})$ (mag)	$M_V(K)_{WB}$ (mag)	$M_V(K)_{Our}$ (mag)
F										
154417		F8.5IV-V	5.5	6.01	0.046	0.0411	4.08	4.0	1.23	2.73
G										
115383	59 Vir	G0V	5.5	5.22	0.079	0.0742	4.57	4.4	1.99	3.51
206860	HN Peg	G0V	10.2	5.94	0.065	0.0666	5.06	4.4	3.28	4.83
218739		G0V		7.20	0.031	0.0298	4.47	4.4	4.00	5.58
20630	κ^1 Cet	G5V	< 15	4.83	0.108	0.1077	4.99	5.1	4.37	5.96
131156 A	ξ Boo A	G8V	3	4.55	0.156	0.1489	5.41	5.5	4.52	6.11
101501	61 UMa	G8V	15	5.33	0.119	0.1115	5.57	5.5	4.75	6.35
K										
190404		K1V		7.24		0.0559	5.98	6.1	6.77	8.43
4628		K2V		5.75	0.143	0.1358	6.41	6.4	7.91	9.61
22049	ϵ Eri	K2V	< 15	3.73	0.304	0.3056	6.16	6.4	5.73	7.36
131511		K2V	4	6.01	0.087	0.0869	5.71	6.4	3.40	4.96
16160		K3V	< 3	5.82	0.129	0.1336	6.45	6.6	4.48	6.07
219134		K3V		5.56	0.146	0.1505	6.45	6.6	4.87	6.47
115404		K3V		6.52		0.0840	6.14	6.6	5.12	6.73
127665	ρ Boo	K3III	15	3.58	0.029	0.0238	0.46	0.3	-1.79	-0.38
131156 B	ξ Boo B	K4V	20	6.90	0.156	0.1489	7.76	7.0	5.86	7.49
201091	61 Cyg A	K5V	2	5.21	0.294	0.2870	7.50	7.4	5.21	6.82
201092	61 Cyg B	K7V	< 3	6.03	0.294	0.2870	8.32	8.1	5.80	7.43

Table 4. Parameters for Barium stars and other giants

HD	Name	T_{sp}	$V \sin i$ (km s^{-1})	V (mag)	π ('')	π * ('')	$M_V(\pi)$ (mag)	$M_V(T_{sp})$ (mag)	$M_V(K)_{WB}$ (mag)	$M_V(K)_{Our}$ (mag)
131873	β UMi	K4 III	< 15	2.08	0.039	0.0238	-1.04	0.00	-1.74	-0.34
163770	θ Her	K1 IIa	< 20	3.86	0.002		-4.63	-2.70	-4.03	-2.69
164349	93 Her	K0.5 IIb	< 15	4.67	0.004	0.0035	-2.61	-2.68	-2.15	-0.75
168532	105 Her	K3 III		5.27	0.002	0.0015	-3.85	0.30	-2.53	-1.14
185958	β Sge	G8 III	< 20	4.37	0.011	0.0091	-0.83	0.80	-2.37	-0.98
198809	31 Vul	G7 III		4.59	0.036	0.0416	2.69	0.85	-0.65	0.79
199939		G9 III		8.00				0.75	1.91	3.42
201657		G9 III		8.10				0.75	4.16	5.74
206778	ϵ Peg	K2 Ib	< 15	2.39	0.006	0.0077	-3.18	-5.90	-4.59	-3.27
211594		K0 (III)		8.09				0.70	0.67	2.15
215665	λ Peg	G8 III	< 20	3.95	0.042	0.0414	2.04	0.80	-0.99	0.44
218356	56 Peg	G8 Ib	< 15	4.76	0.006	0.0018	-3.96	-6.10	-3.55	-2.20

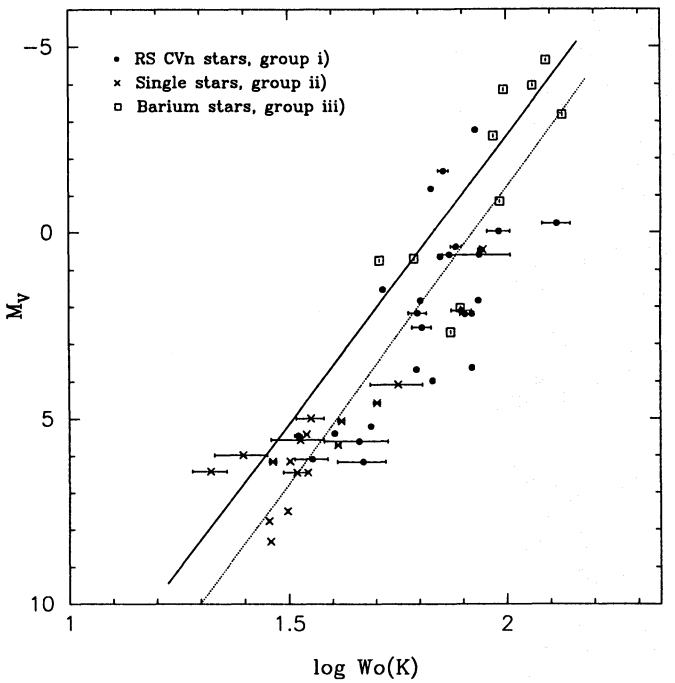

Fig. 2. (log W_0, M_V) diagram. The solid line is the Wilson-Bappu relation by Lutz (1970) and the dotted line corresponds to the linear best fit to our data. Different symbols are used to represent the stars belonging to group i), ii), and iii)

Later, Wilson (1967), using 65 stars with accurate trigonometric parallaxes, obtained the following relationship:

$$M_V = -14.89 \log W_0(K) + 27.51, \quad (4)$$

that agreed very well with the Sun-Hyades calibration. Lutz (1970) obtained an improved regression line using photoelectric magnitudes and a different least-squares technique:

$$M_V = -15.55 \log W_0(K) + 28.49. \quad (5)$$

In Fig. 2 we plot the relation between the trigonometric absolute magnitude, $M_V(\pi)$, and the logarithm of the corrected Wilson-Bappu width, $W_0(K)$, expressed in km s^{-1}. Different symbols are used to represent stars belonging to groups i), ii), and iii). When we have several spectra for the same star the average value of $W_0(K)$ is plotted, and the error bar represents the standard deviation. The solid line is the Wilson-Bappu relation given in (5). This figure shows that, despite the scatter of points around the WB relation, our values of $W_0(K)$ are larger than expected from the WB law. We have also found that there is not a systematic difference among the behaviour of stars belonging to different groups. The scatter can be mainly due to the uncertainties in the trigonometric parallaxes and in the measurements of $W_0(K)$, particularly for stars with very weak Ca II K emission lines. However other sources for this scatter are analysed in the next section. The dotted line shows the linear regression to our data determined with the method of the bisector of the two ordinary least-squares lines described by Isobe et al. (1990):

$$M_V = -16.01 \log W_0(K) + 30.79 \quad (r = 0.88). \quad (6)$$

Where, r, is the linear correlation coefficient. This relationship presents a slope very similar to the relationship of Lutz (1970) but it shows a difference in the constant term of 2.3 mag.

In Tables 2, 3 and 4 we give for each star the absolute magnitudes $M_V(K)_{WB}$ obtained from our measured widths, using the WB relation given in Eq. (5), and the ones obtained from our fit (Eq. (6)), $M_V(K)_{Our}$.

4. Which parameters affect the Wilson-Bappu relation?

4.1. The intensity effect

Glebocki & Stawikowski (1978) found that stars with strong emission intensities, I_K, have systematically lower absolute magnitudes than resulted from the Wilson Bappu relation. I_K is the Wilson eye-estimate scale 0-5, where 0 denote the lack of emission, and 5 means that the intensity is equal to, or greater than, the neighbouring continuum. These authors proposed that an additional factor proportional to the emission strength, I_K, must be introduced into Wilson-Bappu's formula to take into account this intensity effect.

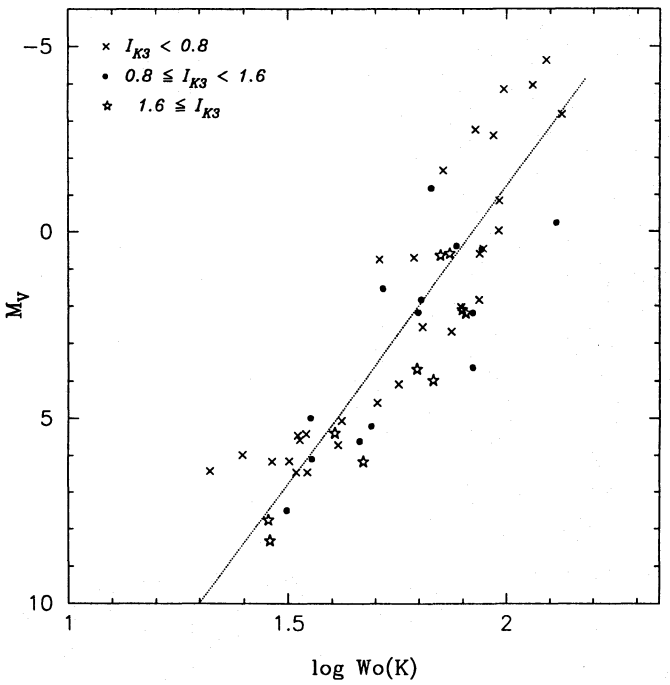

Fig. 3. (log W_0, M_V) diagram as a function of the intensity I_{K_3} We represent with different symbols stars with different values of I_{K_3}. The dotted line shows the linear best fit to our data, Eq. (6)

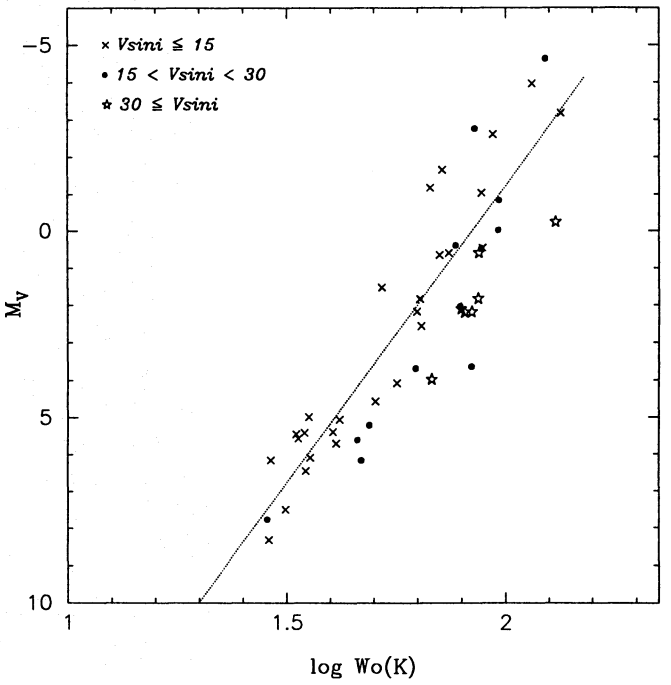

Fig. 4. (log W_0, M_V) diagram as a function of the projected rotational velocity, Vsin i. We represent with different symbols stars with different values of Vsin i. The dotted line shows the linear best fit to our data, Eq. (6)

On the other hand, White & Livingston (1981) and Sivaraman et al. (1987) found a small but significant increase of W_0 with solar activity (0.04 Å), and that the plage profiles have large W_0 as compared with the quiet Sun profile. Recently, García-López et al. (1992) noted a relationship between the flux variability and the width variability of H emission line in late-type stars.

Some of the chromospherically active binary systems studied by us present very strong Ca II K emission lines. The largest value of I_{K_3}, measured in our sample, is 4.6, i.e the emission peak is 4.6 times the pseudocontinuum level at 3950.5 Å, and the lowest is about 0.2, which corresponds to a solar spectrum dominated by plages.

In order to investigate the influence of the intensity effect on the WB width of the stars of our sample, we have plotted in the WB diagram (Fig. 3) with different symbols the stars included in three different intervals of the emission intensity I_{K_3}. The stars with the largest intensities ($I_{K_3} \geq 1.6$) show larger values of W_0(K), all being placed to the right of the WB relationship, and the following regression line can be fitted:

$$M_V = -14.80 \log W_0(K) + 29.87 \quad (r = 0.94). \tag{7}$$

The stars whose intensities are included in the interval ($0.8 \leq I_{K_3} < 1.6$) in general present also larger values of W_0 those expected for the WB relation but the scatter in this case is larger. Finally, the stars with the lowest values of emission intensities ($I_{K_3} < 0.8$) spread to both sides of the WB relation.

In this sense, when we studied $\Delta M_V(W_0)$ (the difference between $M_V(\pi)$ and $M_V(K)_{Our}$) as a function of I_{K_3} we found that $\Delta M_V(W_0)$ is larger and with positive value for larger values of I_{K_3} but a clear trend is not found.

4.2. *Influence of rotational broadening*

Bielicz et al. (1985) studied the influence of rotational broadening on the width of the Ca II K emission line and they have shown that the full width at half maximum (FHWM), W_0, increases linearly with Vsin i for low rotational velocities (up to 15 km s^{-1}) and for larger velocities the increase of W_0 becomes strongly non-linear.

The influence of rotational broadening above mentioned must be important in rapidly rotating systems, as the chromospherically active binary systems analysed in this work, and could be one of the causes of the scatter observed in the (log W_0(K), M_V) diagram.

The Vsin i values adopted for the stars of this sample are given in Tables 2, 3 and 4 and have been taken from CABS II (group i)), the "Bright Star Catalogue" (groups ii) and iii)) and, in some cases, from the "Revised Catalogue of Rotational velocities of the Stars" (Uesugi & Fukuda 1982). In few cases only upper limits of Vsin i are available, nevertheless all are included in the analysis.

The rotational broadening effect can be seen in Fig. 4, where we have denoted with different symbols stars with different values of Vsin i. Stars with low Vsin i (Vsin $i \leq 15$ km s^{-1}) are leftwards and stars with high Vsin i (Vsin $i \geq 30$ km s^{-1}) are rightwards in the (log W_0(K), M_V) diagram.

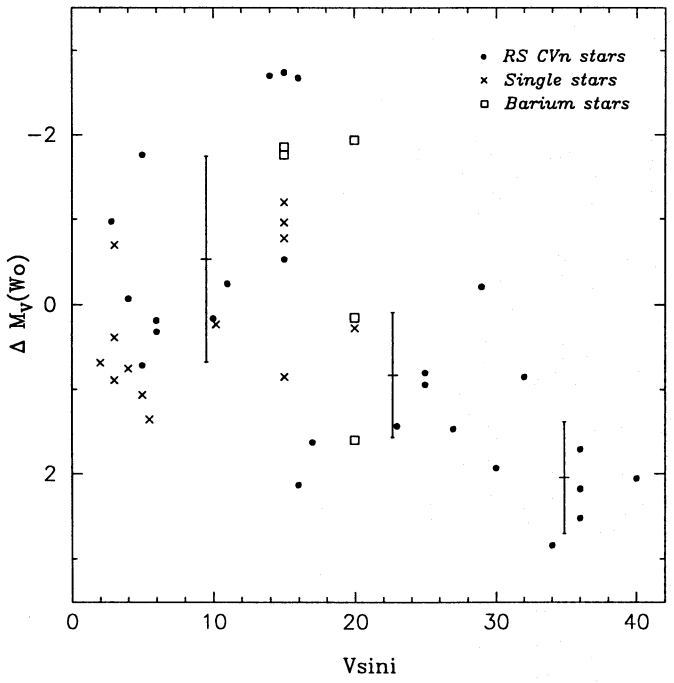

Fig. 5. Difference between trigonometric absolute magnitude and the absolute magnitude derived from the W_0 value by using our fitted WB relation, ΔM_V versus Vsin i. Different symbols are used to represent the stars belonging to group i), ii) and iii)

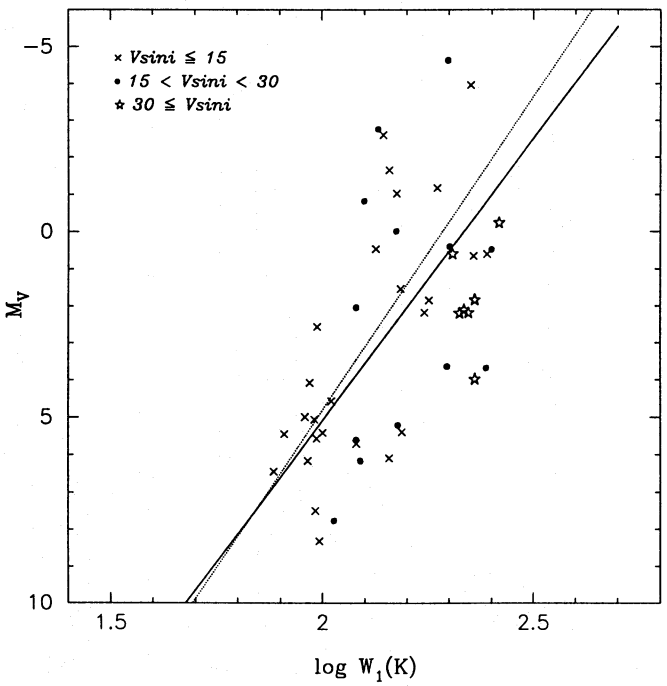

Fig. 6. ($\log W_1$, M_V) diagram as a function of the projected rotational velocity, Vsin i. The solid line is the relation obtained by Engvold & Rygh (1978), and the dotted line shows the linear best fit to our data, Eq. (9)

When we plot $\Delta M_V(W_0)$ versus Vsin i (Fig. 5) we find that the differences are larger and with positive values for larger values of Vsin i, but a scatter is present, particularly for low values of Vsin i. In this figure vertical bars represent the standard deviation of the average $\Delta M_V(W_0)$ for the three Vsin i intervals considered.

In conclusion, we claim that in very active stars the influence of the rotational broadening in the WB relation is more remarkable than the effect of the emission intensity.

5. W_1 width-luminosity correlation

The line width W_1 is physically significant because it is a rough measure of the location of the stellar temperature minimum in line optical depth units. Ayres et al. (1975) presented evidence for a width-luminosity correlation of $W_1(K)$ and they converted their empirical relation to a more useful form, obtaining W_1 as a function of stellar surface gravity, g, and effective temperature, T_{eff}. Later, Engvold & Rygh (1978) found that the $W_1(K)$ values of a sample of giants and supergiants fit the following width-luminosity correlation:

$$M_V \approx (-15.2)\log W_1(K) + const \quad (r = 0.89). \tag{8}$$

The following relation between $\log W_1(K)$ and the trigonometric absolute magnitude, $M_V(\pi)$, for the stars of our sample, has been obtained:

$$M_V = (-16.91)\log W_1(K) + 38.63 \quad (r = 0.60), \tag{9}$$

when $W_1(K)$ is expressed in km s^{-1} and is corrected from the instrumental width in the same way as $W_0(K)$.

In Fig. 6 we have plotted with different symbols stars with different values of Vsin i. The solid line is the relation obtained by Engvold & Rygh (1978) and the dotted line shows the linear best fit to our data (Eq. 9). A clear separation among stars in the three intervals of Vsin i is not found. This conclusion is in agreement with Bielicz et al. (1985) who found that the W_1 width is less influenced by the rotation than W_0.

However, if we plot $\Delta M_V(W_1)$ (the difference between $M_V(\pi)$ and the absolute magnitude derived from above relation (9)) versus I_{K_3}, a trend to increase $\Delta M_V(W_1)$ with I_{K_3} is observed with a larger scatter for lower I_{K_3} (Fig. 7). In this figure, vertical bars represent the standard deviation of the average $\Delta M_V(W_1)$ for the three I_{K_3} interval considered.

So we conclude that the intensity effect can be ascribed as the main cause of the scatter in the $W_1(K)$ luminosity relation. This conclusion is clearly seen in Fig. 8 (the same diagram as Fig. 6) where we use different symbols to represent stars with different values of I_{K_3}. The stars with the largest intensities ($I_{K_3} \geq 1.6$) show larger values of $W_1(K)$, and the dashed line represents the linear regression for the stars of this group:

$$M_V = (-16.80)\log W_1(K) + 41.88 \quad (r = 0.92). \tag{10}$$

The stars with intermediate and low intensities show the following fits respectively (dotted-dashed and dotted lines in Fig. 8)

$$M_V = (-18.13)\log W_1(K) + 42.61 \quad (r = 0.83), \tag{11}$$

Table 5. CaII H and K line parameters (RS CVn and BY Dra stars)

HD	Name	φ		W(K) (Å)	W_1(K) (Å)	$I_{K_{1V}}$	$I_{K_{1R}}$	I_{K_3}	W(H) (Å)	W_1(H) (Å)	$I_{H_{1V}}$	$I_{H_{1R}}$	I_{H_3}	W(Hϵ) (Å)	O
1833	BD Cet	0.90	-	1.15	2.62	0.20	0.20	0.96	1.04	1.98	0.29	0.30	0.95		8
4502	ζ And	0.29	C	1.20	3.04	0.27	0.25	0.72	1.16	2.49	0.30	0.34	0.74		7
.	.	0.69	C	1.22	2.65	0.23	0.21	0.79	1.16	2.53	0.29	0.31	0.78		8
5516	η And	0.62	-	1.01	1.87	0.13	0.13	0.20	1.02	1.64	0.17	0.15	0.22		8
7672	AY Cet	0.61	C	0.77	2.04	0.21	0.20	0.88	0.76	1.69	0.24	0.25	0.86		8
8357	AR Psc	0.33	H	0.64	1.98	0.26	0.24	1.45	0.60	1.94	0.28		1.38	0.86	2
.	.	0.39	H	0.58	1.76	0.26	0.29	1.50	0.61	1.91	0.29		1.48	1.10	2
.	.	0.67	H	0.63	2.04	0.27	0.26	1.51	0.63	1.88	0.33		1.41	0.88	2
12545	-	-	-	0.90	3.22	0.37	0.32	4.63	0.92	3.10	0.39		4.60	1.25	8
17433	VY Ari	0.17	-	0.64	2.05	0.23	0.26	2.57	0.60	1.74	0.30		2.40	0.87	8
32357	12 Cam	0.51	-	1.22	3.31	0.34	0.35	1.66	1.10	3.37	0.41	0.43	1.66		2
.	.	0.52	-	1.24	3.32	0.36	0.36	1.66	1.13	3.40	0.40	0.44	1.63		2
.	.	0.57	-	1.23	3.55	0.34	0.34	1.55	1.14	3.48	0.37	0.46	1.54		2
.	.	0.57	-	1.19	3.17	0.33	0.33	1.41	1.12	3.28	0.36	0.43	1.41		2
37824	V1149 Ori	0.19	C	1.05	3.23	0.28	0.28	1.69	0.99	2.66	0.35		1.73		9
.	.	0.19	C	1.07	3.26	0.28	0.29	1.68	0.96	2.89	0.36		1.77		9
62044	σ Gem	0.82	-	1.03	2.60	0.23	0.24	1.07	0.94	2.10	0.29	0.34	1.08		4
.	.	0.82	-	1.05	2.40	0.22	0.23	1.06	0.94	2.23	0.27	0.33	1.07		4
.	.	0.92	-	0.99	2.49	0.22	0.23	1.08	0.91	2.03	0.28	0.32	1.10		4
.	.	0.41	-	1.04	3.05	0.23	0.24	1.37	0.93	2.46	0.30	0.37	1.35		7
-	DM UMa	0.85	-	0.98	3.04	0.43	0.37	2.80	1.05	3.41	0.49		2.63	1.56	9
98230	ξ UMa(B)	0.49	C	0.48	1.08	0.19	0.19	0.43	0.45	1.13	0.22	0.22	0.42		4
113816	-	-	-	1.14	2.80	0.22	0.15	2.66	1.10	2.94	0.22		2.20		9
136905	GX Lib	0.36	C	1.29	2.89	0.24	0.24	0.83	1.14	2.50	0.34	0.34	0.91		6
.	.	0.44	C	1.02	2.46	0.20	0.22	0.75	0.96	2.27	0.31	0.33	0.81		6
.	.	0.83	C	1.09	2.78	0.22	0.20	0.75	1.02	2.67	0.28	0.29	0.75		9
153751	ϵ UMi	0.43	C	1.28	1.98	0.22	0.21	0.34	1.24	1.61	0.27	0.25	0.36		6
160538	DR Dra	-	C	0.86	2.36	0.21	0.24	1.42	0.78	2.00	0.28	0.35	1.53		6
166181	V815 Her	0.68	H	0.67	1.99	0.26	0.27	1.08	0.77	1.49	0.28	0.29	0.91	0.85	5
175306	o Dra	0.66	-	1.42	1.74	0.13	0.12	0.24	1.85	1.57	0.17	0.15	0.25		6
175742	V775 Her	0.04	H	0.47	1.61	0.21	0.24	2.83	0.44	1.48	0.24		2.38	0.74	5
.	.	0.06	H	0.51	1.40	0.18		2.85	0.44	1.45	0.19		2.62	1.06	5
.	.	0.37	H	0.49	1.62	0.21	0.24	2.60	0.47	1.21	0.26		2.50	0.69	5
.	.	0.40	H	0.47	1.52	0.24	0.28	2.69	0.44	1.31	0.30		2.42	0.65	5
.	.	0.07	H	0.65	1.96	0.24	0.28	2.10	0.63	1.48	0.26		1.78	0.83	5
178450	V478 Lyr	0.40	H	0.53	1.60	0.27	0.33	1.63	0.47	1.49	0.30		1.53	0.51	5
.	.	0.85	H	0.65	1.44	0.27	0.26	1.26	0.56	1.74	0.27		1.20	0.56	5
.	.	0.77	H	0.72	1.72	0.26	0.24	0.95	0.76	1.68	0.25		0.89		5
179094	V1762 Cyg	0.45	-	0.90	2.46	0.21	0.22	1.20	0.85	1.98	0.26	0.29	1.21		6
185151	V1764 Cyg	-	C	1.72	3.44	0.32	0.32	0.93	1.54	3.17	0.36	0.30	0.95		6
206301	42 Cap	0.18	-	0.87	1.29	0.16	0.16	0.32	0.89	1.45	0.16	0.17	0.29		5
209813	HK Lac	0.89	C	0.95	2.99	0.27	0.26	1.98	0.87	2.58	0.34	0.47	2.06	1.07	6
213389	V350 Lac	0.50	-	1.11	2.91	0.24	0.23	1.19	1.01	2.48	0.29	0.34	1.22		6
216489	IM Peg	0.45	C	1.09	2.80	0.30	0.31	2.01	0.97	2.80	0.29	0.39	1.83		5
.	.	0.65	C	1.02	2.89	0.27	0.27	1.59	0.92	2.58	0.33	0.43	1.70		6
222107	λ And	0.56	-	0.82	2.21	0.19	0.19	1.13	0.78	1.77	0.24	0.26	1.20		6
.	.	0.10	-	0.87	2.39	0.22	0.21	1.23	0.79	2.06	0.29	0.31	1.31		7

$$M_V = (-20.90)\log W_1(K) + 45.33 \quad (r = 0.75). \qquad (12)$$

Therefore, we can conclude that the W_1 width-luminosity correlation is strongly influenced by the intensity effect but it is less influenced by rotational broadening than the W_0 width-luminosity correlation.

6. Relation between Ca II H and K line widths and intensities

6.1. The relation between $W_1(K)$ and I_{K_3}

Ayres (1979) showed that the separation of the K_1 minima, W_1, increases with increased chromospheric emission (I_{K_3}). This behaviour is in agreement with the results for the Sun reported by White & Livingston (1981) and Sivaraman et al. (1987), with the results obtained by Glebocki & Stawikowski (1980) for 70 F, G, K and M type stars and with the results for a sample of nearby solar type stars (G0-G5) reported by Pasquini (1992).

We analyse the K_1 separation, W_1(K), for the stars of the sample as a function of the K_3 intensity, I_{K_3}, which is shown in Fig. 9 together with the values of the sample of Pasquini (1992). The scatter observed in this figure is due to the errors in the K_1 positioning, which are larger in low active stars, and to the possible effects produced in the line core by the WB width, W_0.

For the low active stars ($I_{K_3} < 0.2$) we can observe that W_1(K) tends to increase steeply when the activity increases. For more active stars ($I_{K_3} \geq 0.2$) the increase of W_1(K) with I_{K_3} tends to become flatter.

A similar conclusion was derived by Pasquini (1992) when he analysed single stars of moderately activity ($I_{K_3} \leq 0.5$). As

Table 6. CaII H and K line parameters (Single active stars)

HD	Name	W(K) (Å)	W_1(K) (Å)	$I_{K_{1V}}$	$I_{K_{1R}}$	I_{K_3}	W(H) (Å)	W_1(H) (Å)	$I_{H_{1V}}$	$I_{H_{1R}}$	I_{H_3}	W(Hϵ) (Å)	O
F													
154417		0.77	1.24	0.17	0.18	0.21	0.88	1.16	0.22	0.21			6
G													
115383	59 Vir	0.69	1.39	0.19	0.19	0.31	0.76	1.18	0.24	0.22	0.35		6
206860	HN Peg	0.58	1.27	0.19	0.19	0.35	0.56	1.12	0.23	0.21	0.35		6
218739		0.61	1.27	0.20	0.19	0.38	0.65	1.29	0.22	0.20	0.35		8
20630	κ^1 Cet	0.59	1.24	0.18	0.19	0.40	0.59	1.30	0.23	0.22	0.38		8
131156 A	ξ Boo A	0.50	1.33	0.20	0.21	0.63	0.49	1.27	0.24	0.21	0.62		6
101501	61 UMa	0.61	1.34	0.18	0.19	0.30	0.67	1.24	0.23	0.21	0.30		9
K													
190404		0.38	0.77	0.12	0.13	0.16							6
4628		0.45	1.00	0.13	0.15	0.29	0.56	1.00	0.20	0.18	0.26		8
22049	ϵ Eri	0.52	1.26	0.19	0.20	0.80	0.48	1.18	0.24	0.23	0.78	0.36	8
131511		0.68	1.63	0.20	0.21	0.52	0.70	1.53	0.25	0.24	0.50		9
16160		0.58	1.07	0.17	0.14	0.26	0.65	0.97	0.21	0.18	0.25		8
219134		0.48	1.05	0.13	0.13	0.24	0.41	0.97	0.17	0.17	0.25		6
115404		0.46	1.07	0.20	0.20	0.80	0.42	1.06	0.26	0.21	0.77		6
127665	ρ Boo	1.23	1.81	0.09	0.09	0.10							9
131156 B	ξ Boo B	0.42	1.41	0.35	0.35	2.51	0.41	1.39	0.39	0.37	2.27	0.47	6
201091	61 Cyg A	0.46	1.28	0.23	0.23	1.09	0.45	1.08	0.30	0.27	1.08	0.37	6
201092	61 Cyg B	0.43	1.31	0.29	0.27	1.97	0.43	1.21	0.33	0.32	1.82	0.46	6

Table 7. CaII H and K line parameters (Barium stars and other giants)

HD	Name	W(K) (Å)	W_1(K) (Å)	W_2(K) (Å)	$I_{K_{1V}}$	$I_{K_{1R}}$	$I_{K_{2V}}$	$I_{K_{2R}}$	I_{K_3}	O
131873	β UMi	1.17	1.98	0.65	0.13	0.13	0.24	0.29	0.23	6
163770	θ Her	1.63	2.61	0.91	0.12	0.18	0.24	0.31	0.23	6
164349	93 Her	1.24	1.84	0.90	0.11	0.11	0.16	0.15	0.11	6
168532	105 Her	1.31	2.12	0.85	0.138	0.15	0.24	0.25	0.17	6
185958	β Sge	1.28	1.66	0.86	0.11	0.11	0.13	0.12	0.10	6
198809	31 Vul	1.00	1.45	0.50	0.14	0.14	0.19	0.18	0.17	6
199939		0.70	1.10	0.47	0.09	0.09	0.12	0.11	0.09	6
201657		0.52	0.71	0.22	0.08	0.09	0.11	0.12	0.11	6
206778	ϵ Peg	1.77	2.75	1.14	0.25	0.24	0.43	0.60	0.14	6
211594		0.83	1.18	0.56	0.12	0.12	0.17	0.16	0.07	6
215665	λ Peg	1.05	1.59	0.79	0.10	0.10	0.12	0.11	0.09	6
218356	56 Peg	1.52	2.95	0.69	0.28	0.28	0.77	0.58	0.57	6

HD	Name	W(H) (Å)	W_1(H) (Å)	W_2(H) (Å)	$I_{H_{1V}}$	$I_{H_{1R}}$	$I_{H_{2V}}$	$I_{H_{2R}}$	I_{H_3}	O
131873	β UMi	1.11	1.68	0.64	0.15	0.15	0.23	0.26	0.22	6
163770	θ Her			0.97	0.17		0.27		0.23	6
164349	93 Her	1.19	1.55	0.85	0.14	0.13	0.17	0.16	0.12	6
168532	105 Her	1.25	1.78	0.79	0.16	0.16	0.24	0.24	0.19	6
185958	β Sge	1.18	1.44	0.90	0.14	0.12	0.15	0.13	0.10	6
198809	31 Vul	0.92	1.24	0.56	0.17	0.15	0.20	0.19	0.18	6
199939		0.90	1.20	0.61	0.13	0.10	0.14	0.12	0.10	6
201657		0.83	1.06	0.58	0.12	0.10	0.13	0.13	0.11	6
206778	ϵ Peg	1.59	2.32	1.15	0.31	0.25	0.43	0.60	0.15	6
211594										6
215665	λ Peg	1.11	1.40	0.86	0.12	0.11	0.13	0.12	0.09	6
218356	56 Peg	1.34	2.55	0.66	0.36	0.36	0.80	0.63	0.64	6

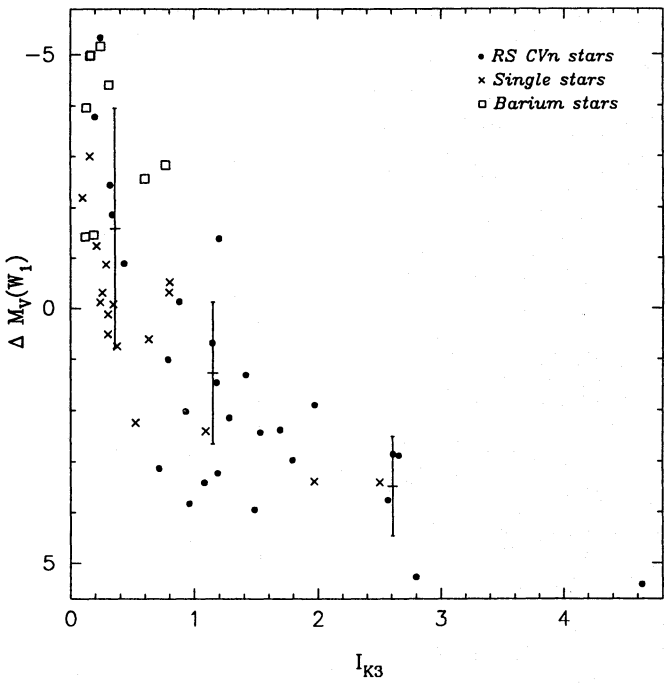

Fig. 7. Difference between trigonometric absolute magnitude and the derived from the W_1 value by using the W_1 width-luminosity relation adjusted by us, ΔM_V versus I_{K_3}. Different symbols are used to represent the stars belonging to group i), ii) and iii)

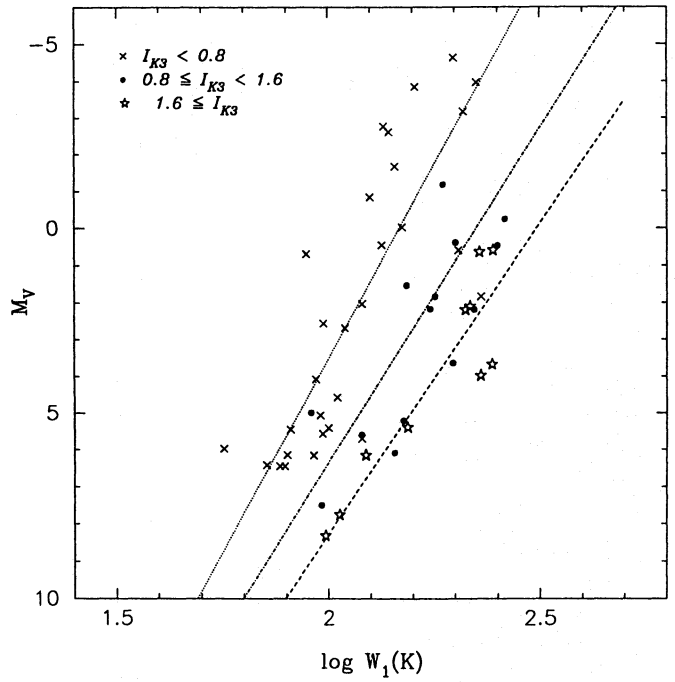

Fig. 8. (log W_1, M_V) diagram as a function of I_{K_3}. We represent with different symbols the stars with different values of I_{K_3}. The three lines correspond to the linear fits in each intensity interval, Eqs. (10), (11) and (12)

can be seen in Fig. 9, if much more active stars are considered a spread of the "flattening" appears. In fact, the relation between $W_1(K)$ and I_{K_3} is affected by the WB width, i.e. there exists a different relation for each value of $W_0(K)$. We have studied this effect by constructing artificial Gaussian emission profiles (with different FWHM = W_0) superimposed on the observed Ca II K absorption line profile. The variation of W_1 with I_{K_3} obtained in this way is shown in Fig. 9 with dotted lines, for three values of W_0 (0.4, 0.9, 1.5).

Moreover, we have also found that the behaviour of the relation between I_{K_1} and I_{K_3} is similar to the described above between $W_1(K)$ and I_{K_3}, i.e. it presents also a flattening for the most active stars and there exits a different relation for each value of $W_0(K)$. On the other hand, the increase of I_{K_1} is also related to the widening of the K_1 minima, $W_1(K)$.

We can conclude that, for low active stars, an increase of I_{K_3} tends to enlarge $W_1(K)$ and to enhance I_{K_1}, while, for high active stars, an increase of activity does not produce strong changes in $W_1(K)$ and I_{K_1}. Although this behaviour is influenced by the WB width, $W_0(K)$.

6.2. *The relation between $W_1(K)$ and $W_0(K)$*

Engvold & Rygh (1978) found that $W_1(K)$ is related with the WB width $W_0(K)$ as follows:

$$log W_1(K) = 0.78 \log W_0(K) + 0.34 \quad (r = 0.91), \tag{13}$$

Cram et al. (1979), Severino (1982) and Marmolino & Severino (1983) found a similar relation.

We also found that $W_1(K)$ is related with the WB width $W_0(K)$ but this relationship is further influenced by the intensity effect. The stars with larger values of I_{K_3} have larger values of W_1 for the same value of W_0 (see Fig. 10). The influence of I_{K_3} in the relation between W_1 and W_0 is in agreement with the above mentioned dependence on W_0 of the relation between W_1 and I_{K_3}.

In Fig. 10 we have superimposed vertical dotted lines representing, for three different values of W_0, the relation between W_1 and I_{K_3} obtained with artificial Gaussian emission profiles, with I_{K_3} ranging from 0.1 to 4.6. This result seems to reflect that does not exist a single valued relation between $W_1(K)$ and $W_0(K)$ and that it is necessary to introduce a correction to take into account the intensity effect.

6.3. *The K/H ratio*

The line widths W_0 and W_1 were also measured for H line emission except in spectra where H was either too weak or blended with the Hε emission line. A trend to larger values of the K line widths respect of the H line widths was found, being the ratio higher in the case of the W_1 width. The following average width ratios were obtained:

$$\frac{W_0(K)}{W_0(H)} = 1.06 \pm 0.09 \quad \text{and} \quad \frac{W_1(K)}{W_1(H)} = 1.12 \pm 0.09. \tag{14}$$

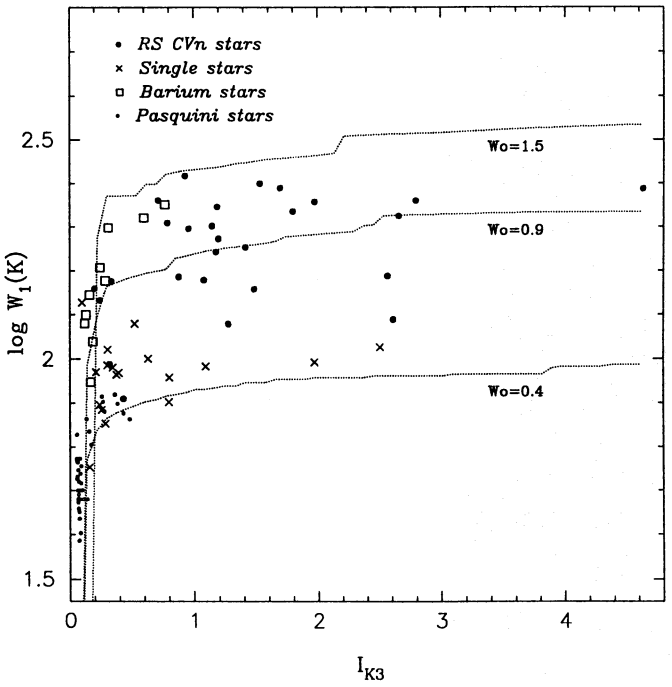

Fig. 9. log W_1 versus I_{K_3} intensity. Dotted lines represent the variation of W_1 with I_{K_3} for three values of W_0 (0.4, 0.9, 1.5) obtained with artificial Gaussian emission profiles. Different symbols are used to represent the stars belonging to group i), ii), iii) and the stars of the sample of Pasquini (1992)

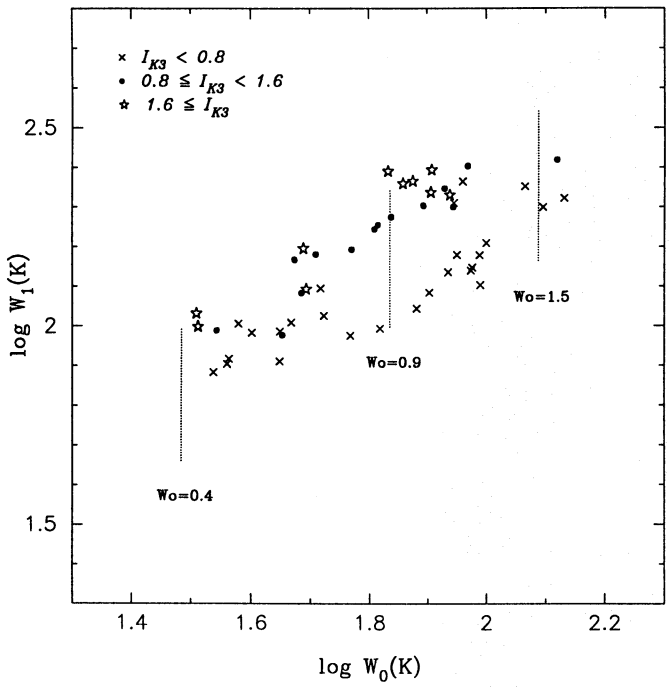

Fig. 10. log W_1 versus log W_0. Dotted lines represent the variation of W_1 with I_{K_3} for three values of W_0 (0.4, 0.9, 1.5) obtained with artificial Gaussian emission profiles. We represent with different symbols stars with different values of I_{K_3}

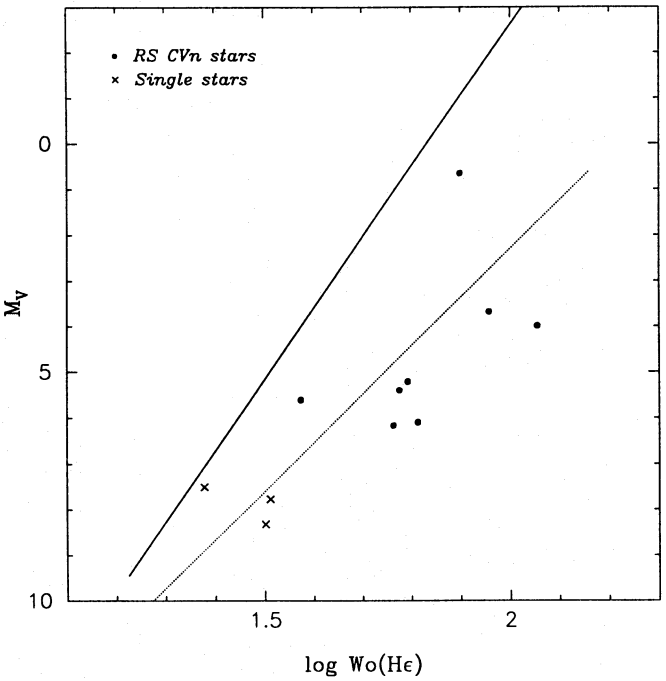

Fig. 11. (log $W_0(H\epsilon)$, M_V) diagram. The solid line is the Wilson-Bappu relation for the K line by Lutz (1970) and the dotted line corresponds to the linear best fit to our Hε line data. Different symbols to represent the stars belonging to group i) and ii) are used

Wilson & Bappu (1957) noted that W_0 width is very similar in the H and K emission lines and, only when the disagreement exceeds 10 per cent, K is measured wider than H. Engvold & Rygh (1978) obtained a W_1 width ratio (W_1(K)/W_1(H) = 1.17 ± 0.06), slightly larger than the determined in this work.

The higher values of K line respect to H line are in agreement with the behaviour of the H and K stellar surface fluxes of a large sample of chromospherically active binary systems studied by Fernández-Figueroa et al. (1993), where the average flux ratio obtained is F_S(K)/F_S(H) = 1.49.

7. Hε emission width-luminosity correlation

The measured Hε line widths, W(Hε) for the 11 stars of the sample which present this line in emission are given in Table 5. In some cases Gaussian fits have been performed in order to separate the Hε line from the Ca II H line.

Although the amount of data is not enough to draw a firm conclusion, a relation between the corrected Hε line width, $W_0(H\epsilon)$, and the absolute magnitude similar to the Wilson-Bappu relationship seems to be present (see Fig. 11). The least squares fit to these data is:

$$M_V = (-10.6)\log W_0(H\epsilon) + 23.5 \quad (r = 0.80). \tag{15}$$

The slope is smaller that in the WB relationship and in general $W_0(H\epsilon)$ is larger than W_0(H), except in some stars in which the Hε emission line is very weak and the errors are largest.

8. Conclusions

We can summarize the results obtained in this paper in the following:

We have found that for very active stars the emissions widths, both $W_0(K)$ and $W_1(K)$, are larger than expected from previously accepted width-luminosity relations.

After analysing the influence of the activity level (the intensity effect, I_{K_3}) and the rotational broadening ($V\sin i$) in the ($\log W_0(K)$, M_V) we find that stars with strong emission intensities, I_{K_3}, and large values of $V\sin i$ present larger values of $W_0(K)$ than resulted from WB relation, being more remarkable the effect of the rotational velocity. On the contrary $W_1(K)$ is strongly influenced by I_{K_3} but the effect of the rotational broadening is lesser.

Therefore we can conclude that both effects must be taken into account when we try to obtain absolute magnitudes using width-luminosity relations in very active and rapidly rotating stars.

The increase of $W_1(K)$ and I_{K_1} with I_{K_3} presents a flattening for the most active stars (larger values of I_{K_3}) which is different for each value of $W_0(K)$. This result confirms, for very active stars, the behaviour observed by other authors in the Sun and in solar type stars.

In order to establish the real influence of the level of activity and the rotational velocity in the Wilson-Bappu width is necessary to obtain high resolution and high S/N ratio spectra for a large number of stars with different levels of activity and with well determined trigonometric parallaxes and rotational velocities. In a near future it will be possible to obtain more accurate $M_V(\pi)$ values from the new trigonometric parallaxes provided by the HIPPARCOS mission.

Acknowledgements. The INT 2.5m on the island of La Palma and the 2.2m telescope at Calar Alto Observatory are operated respectively, by the Royal Greenwich Observatory at the Spanish Observatorio del Roque de Los Muchachos (Instituto de Astrofísica de Canarias), and the Max Planck Institut für Astronomie at the Centro Astronómico Hispano-Alemán of Calar Alto (Almería, Spain). We want to express our gratitude to the staff of both Observatories for their help during the observations. This work has been supported by the Universidad Complutense de Madrid and the Spanish Dirección General de Investigación Científica y Técnica (DGICYT) under grant PB91-0348.

References

Athay R.G., Skumanich A., 1968, ApJ 152, 141
Ayres T.R., 1979, ApJ 228, 509
Ayres T.R., Linsky J.L., Shine R.A., 1975, ApJ 195, L121
Bielicz E., Glebocki R., Sikorski J., 1985, A&A 153, 269
Cornide M., Fernández-Figueroa M.J., De Castro E., Armentia J.E., Reglero, V., 1992, AJ 103, 1374
Cram L.E., Krikorian R., Jefferies J.T., 1979, A&A 71, 14
Engvold O., Rygh B.O., 1978, A&A 70, 399
Fernández-Figueroa M.J., Montes D., De Castro E., Cornide M., 1993, ApJS (Accepted)
Fosbury R.N.E., 1973, A&A 27, 129
García-López R.J., Crivellari L., Beckman J.E., Rebolo R., 1992, A&A 262, 195
Glebocki R., Stawikowski A., 1978, A&A 68, 69
Glebocki R., Stawikowski A., 1980, Acta Astron. 30, 285
Hoffleit D., Jaschek C., 1982, The Bright Star Catalogue (4th ed.: New Haven: Yale University Press)
Isobe T., Feigelson E.E., Akritas M.G., Babu G.J., 1990, ApJ 364, 104
Linsky J.L., Avrett E.H., 1970 PASP 82, 169
Linsky J.L. et al., 1979, ApJS 41, 47
Lutz T.E., 1970, AJ 75, 1007
Lutz T.E., Pagel B.E.J., 1982, MNRAS 199, 1101
Marmolino G., Severino G., 1983, A&A 127, 33
Neckel H. 1974, A&A 35, 99
Pasquini L., 1992, A&A 266, 347
Reimers D., 1973, A&A 24, 79
Severino G., 1982, A&A 109, 90
Sivaraman K. R., Singh J., Bagare S.P., Gupta S.S., 1987, ApJ 313, 456
Scharmer G.B., 1976, A&A 53, 341
Schmidt-Kaler T., 1982, in Landolt-Börnstein, Vol. 2b, ed K. Schaifers, H.H. Voigt (Heidelberg: Springer)
Stencel R.E., 1977, ApJ 215, 176
Strassmeier K.G., Fekel F.C., Bopp B.W., Dempsey R.C., Henry G.W. 1990, ApJS 72, 191
Strassmeier K.G., Hall D.S., Zeilik M., Nelson E., Eker Z., Fekel F.C., 1988, A&AS 72, 291 (CABS I)
Strassmeier K.G., Hall D.S., Fekel F.C., Scheck M., 1993, A&AS 100, 173 (CABS II)
Thomas R.N., 1973, A&A 29, 298
Uesugi A., Fukuda I., 1982, Revised Catalogue of Stellar rotational velocities, (Kyoto University, Kyoto, Japan)
Van Altena et al., 1991, Yale University Observatory (The General Catalogue of Trigonometric Parallaxes, preliminary version)
White O.R., Livingston W.C., 1981, ApJ 249, 798
Wilson O.C., Bappu M.K.V., 1957, ApJ 125, 661
Wilson O.C., 1959, ApJ 130, 449
Wilson O.C., 1967, PASP 71, 46
Wilson O.C., 1978, ApJ 226, 379

This article was processed by the author using Springer-Verlag LaTeX A&A style file version 3.